URSI AP-RASC 2019, New Delhi, India, 09 - 15 March 2019

Circuit Model for a Textile Linear-to-Circular Polarizer using Swastika-Shaped FSS

Hidayath Mirza[1,2], Ping Jack Soh* [1], Toufiq Md Hossain[1], Rais Sheikh Ahmad[1,2], Azremi Abdullah Al-Hadi[1], Mohd Faizal Jamlos[1], and Sen Yan[3]

(1) Advanced Communication Engineering (ACE) CoE, School of Computer and Communication Engineering, Universiti Malaysia Perlis (UniMAP), Pauh Putra Campus, 02600 Arau, Perlis, MALAYSIA.

(2) Dept. of Electrical Engineering, College of Engineering, Jazan University, P. O. Box 706, Jazan 45142, KINGDOM OF SAUDI ARABIA.

(3) School of Electronics and Information Engineering, Xi'an Jiaotong University, Xi'an, Shaanxi, 710049, CHINA.

Abstract

A circuit model for a flexible linear-to-circular polarizer is proposed. This linear-to-circular polarizer is designed based on the concept of Frequency Selective Surface (FSS) unit cells on one side and a rectangular-shaped conductive strip (CS) on its reverse side. The overall polarizer is implemented on a felt substrate, whereas ShieldIt Super conductive textile is used to form the conductive elements for operation in the S-band. Its principle of operation and its interaction with different orthogonal polarized wave components are first presented, followed by the generation and study of the surface currents to understand the waves in different polarizations. This study is summarized in the form of an equivalent circuit model. To further assess this model, the textile-based polarizer is then simulated using full wave simulations and compared to the results obtained from the proposed circuit model. Both results indicated satisfactory agreement in terms of transmission coefficient. Further analysis of the proposed polarizer using full wave simulations indicated promising results in terms of conversion efficiency and axial ratio. A fractional bandwidth of 7.35 %, operating from 2.36 to 2.55 GHz and an axial ratio of 1.4 dB indicated its operation in the S-band.

1. Introduction

Placing a polarizer in front of a linearly polarized (LP) antenna array to achieve circular polarization (CP) is a simpler alternative in comparison to the full technical effort to design independent high gain CP antennas [1]. This makes such linear-to-circular polarizers popular for different applications. An efficient method in realizing these polarizers is by using FSS unit cells. Different shapes of these FSSs are in the form of loops, meander lines, dipoles [2]-[3]; or other metamaterial-based resonators [4]-[5]. Their operating frequencies include the Ka-band [7], X-band [1], [5], [7]-[8] and several other frequency bands [4]-[5], catering to different applications. However, there is very limited researches on S-band flexible linear-to-circular polarizers, besides an initial work in [3]. These planar structures are generally made using high density materials, which makes these planar array of unit cells rigid. Moreover, they also require implementation in a multi-layered configuration. This typically results in the complex structure, increased size/thickness, and potential cost inefficiency. Conversely, lightweight and flexible textile materials popular in applications such as wearable devices can be realistic alternatives [9].

This manuscript presents a new equivalent circuit model for a linear-to-circular polarizer implemented in a single layered topology, using textiles. The next section describes its theory of operation and its design approach. This is followed by the proposed circuit model and the validation of its performance against the simulated and measured PDMS and textile polarizer in flat condition. These are performed in terms of conversion efficiency, 3dB axial ratio (AR) and fractional bandwidth, which is defined within the 90 % conversion efficiency limits. Finally, Section 4 concludes the findings obtained from the proposed circuit model and its evaluation.

2. Design Principle and Operation

To ensure the generation of CP waves from the polarizer, the criteria in equations (1) and (2) [2], [10] need to be fulfilled:

$$|E_x^t| = |E_y^t| \tag{1}$$

$$\left[\Phi_{E_x^i} + \Phi_{T_x}\right] - \left[\Phi_{E_y^i} + \Phi_{T_y}\right] = \pm n\frac{\pi}{2} \tag{2}$$

with Φ representing the phase of E_x^t and E_y^t, the two orthogonal components of the transmitted electric fields from the polarizer. Meanwhile, $T_x(= E_x^t/E_x^i)$ and $T_y(= E_y^t/E_y^i)$ are the transmission coefficients for E_x^i and E_y^i, which represent the decomposed orthogonal components of the electric field E^i incident on the polarizer.

Further simplification of equations (1) and (2) using $|E_x^i| = |E_y^i|$ and $\Phi_{E_x^i} = \Phi_{E_y^i}$, they can be then written as follows:

$$|T_x| = |T_y| \tag{3}$$

$$\Phi_{T_x} - \Phi_{T_y} = 2n\pi \pm n\frac{\pi}{2} \tag{4}$$

indicating that phase difference between T_x and T_y must be 90º or its odd multiple. A linear-to-circular polarizer is assessed using conversion efficiency and axial ratio using equation (5) and (6), respectively. They are listed as follows:

$$\eta_{conv} = \frac{(abs(C_-)^2 - abs(C_+)^2)}{(abs(C_-)^2 + abs(C_+)^2)} \times 100 \tag{5}$$

$$\mathrm{AR} = \sqrt{\frac{|T_y|^2 + |T_x|^2 + |T_y^2 + T_x^2|}{|T_y|^2 + |T_x|^2 - |T_y^2 + T_x^2|}} \tag{6}$$

where the circular conversion coefficient of the right-handed circular polarization (RHCP) wave and left-handed circular polarization (LHCP) wave, are represented by C_- and C_+, respectively [10]-[11].

The proposed swastika-shaped polarizer unit cell topology is shown in Figure 1. In the front plane, it consists of a conductive strip (CS) located parallel to the $x-$axis, whereas in the reverse plane, a swastika-shaped unit element is placed at an angle of $\alpha = 45^\circ$ relative to the $+x-$axis. The main function of the swastika-shaped structure in this work is to control capacitance in the transmitted electric field, E^t, and the inductive characteristic on other components.

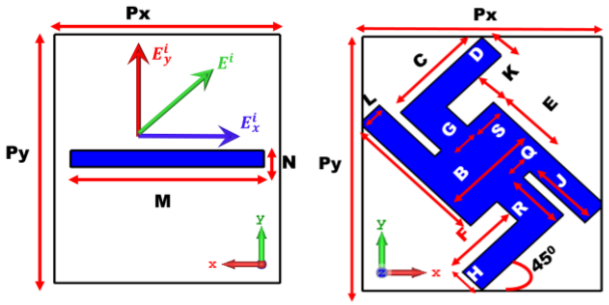

(a) (b)

Figure 1. The proposed swastika-shaped linear to circular polarizer FSS unit cell sized at (P_x x P_y) = 51.7 mm × 59.8 mm (a) front plane, (b) reverse plane. The optimized parameters are: A = 33, B = 24, C = 25, D = 6, E = F = 17, G = 8, H = 6, J = 17, K = 6.5, L = 6, M = 44.3, N = 4, Q = 2, R = 12.5, and S = 8 (all dimensions in mm).

As aforementioned, the proposed polarizer is realized on a felt substrate with a relative permittivity (ε_r) of 1.44 for felt, while ShieldIt features a conductivity of 1.18 x 10^5 S/m with 0.17 mm of thickness. The polarizer was designed with CST Microwave Studio [12] using the unit cell boundary condition in the x- and y-directions. The adaptive meshing in the frequency domain solver is used for these analyses.

To further explain the operation principles of the polarizer, its surface current distribution is first generated as illustrated in Figure 2. It is seen that the x-polarized incident waves coupled to the CS. Meanwhile, the swastika-shaped structure partially modifies the incident waves from being x-directed to being y-directed. On the other hand, the y-polarized incident wave only partially excite the CS, subsequently causing phase difference between the two transmitted orthogonal electric field components, E_x^t and E_y^t.

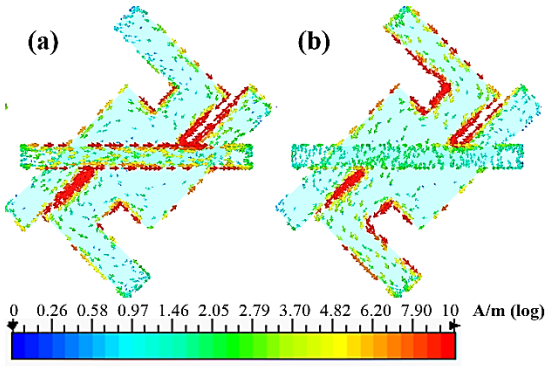

Figure 2. Surface current distribution of the polarizer at 2.45 GHz for the (a) x-polarized and (b) y-polarized incident electric fields.

3. Results and Discussion

The proposed equivalent circuit model is illustrated in Figure 3, with their x- and y-directed field components represented by the x and y subscripts. Parameters $R_{TL_{subs}}$ represents the substrate characteristics and R_{UC} represents the overall resistance of the unit cell. On the other hand, the capacitance and inductance for the CS and swastika-shaped structure are represented by C_x, C_y, L_x and L_y, where their directions are indicated by their subscripts.

The effects of the gap and length variations on the characteristics of the polarizer is first studied. From the findings in [13]-[14], it can be deduced that the capacitance varies proportionally with the width of the gap channel, and inversely proportional to the gap. The larger the width, R, and smaller the gap, Q, as illustrated in Figure 1(b) results in increased capacitance. Meanwhile, the smaller the width, S and the larger the gap channel, K, brings about a decrease in the capacitance in the y-direction, E_y^i Moreover, the longer length of the swastika structure in the $y-$ direction induces additional inductance in the $y-$directed electric field component. On the other hand, the length of the transmission line determines the inductance from this section.

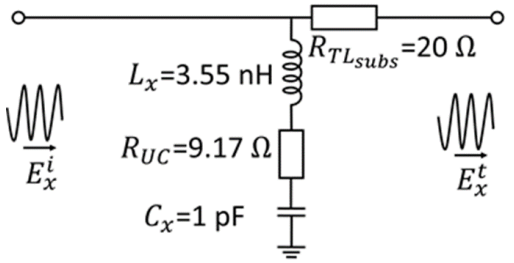

(a)

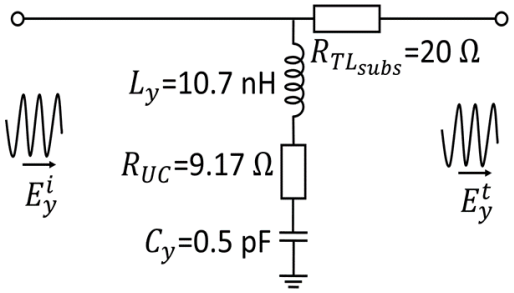

(b)

Figure 3. The proposed equivalent circuit model of the polarizer for the (a) *x*-polarized and (b) *y*-polarized electric fields.

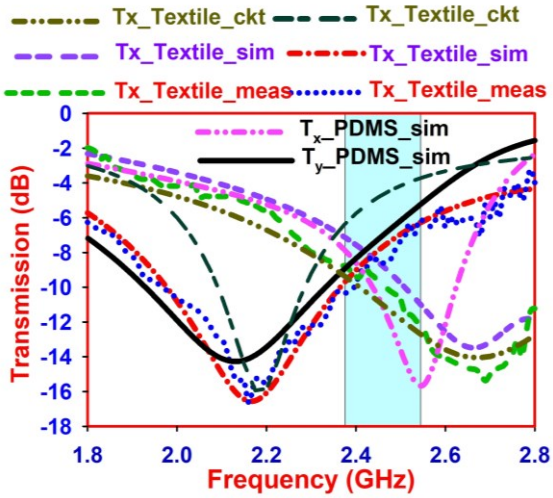

Figure 4. Transmission coefficients of the proposed polarizer obtained from the proposed circuit model and the full wave simulations.

This results in the larger value of C_x relative to its orthogonal counterpart, C_y. Conversely, the inductance characteristic is designed by lengthening L_y to be longer than L_x to generate larger inductance on E_y^i compared to E_x^i. This consequently causes the phase of E_x^t to lead the phase E_y^t. The optimization of the inductance performed by tuning the length, the width and gap of the channels to ensure the criteria for circular polarization is met. The CS in the front plane adds inductance for the E_x^t parallel to the strip, and couples the incident wave to this strip. This enables further tuning of the polarizer without compromising its overall size. To corroborate the accuracy of proposed circuit model, Advance Design System (ADS) software is used to simulate the circuit, and the resulting values are presented in Figure 3. In the circuit simulations, the higher capacitance shifts the transmission coefficients upwards to the higher frequencies and vice versa.

Finally, the full wave simulation results are compared with the results obtained from the proposed equivalent circuit model and presented in Figure 4. The result analysed at 2.4 GHz indicated a conversion efficiency of 95.78 % and a phase difference of 80.2º. Besides that, these results indicated the polarizer's operation from 2.36 to 2.54 GHz, judging from the 90 % conversion efficiency borders. This translates into a fractional bandwidth BW_{CE} is 7.35 % when studied using full wave simulations. This motivates the further investigation of the textile prototype via fabrication and experimental study.

4. Conclusion

In this paper, an equivalent circuit model is proposed for an innovative S-band linear-to-circular polarizer made fully using textiles. The textile materials, felt and ShieldIt, are commercially-available, lightweight and cost-efficient, and are used to ensure polarizer's flexibility, weight and design simplicity. The criteria for circular polarization and operating principles of the polarizer is first presented. This is followed by the full wave analysis of the overall structure and the generation of its surface current distribution. From this, the behaviour of the waves is studied in detail and the equivalent circuit model is then proposed. Comparison between the transmission coefficients obtained from this circuit model and the full wave simulations indicated good agreements. Simulations performed for this textile-based polarizer indicated promising results, with more than 95 % of conversion efficiency, and an AR of 1.4 dB in the S-band. It also exhibited a fractional bandwidth of 7.35 %, operating with more than 90 % of conversion efficiency from 2.36 to 2.55 GHz.

Acknowledgements

This project is supported in part the Research Foundation Flanders (F.W.O.) Postdoctoral Fellowship (No. 12O1217N) and the Malaysian Ministry of Education (MoE) Prototype Development Research Grant Scheme (PRGS) (ref: PRGS/2/2015/ICT06/UNIMAP/02/1). The authors would also like to acknowledge the technical contributions by Mr. Abdul Halim Lokman and Dr. Rizwan Khan.

References

1. M. Fartookzadeh and S. H. M. Armaki, "Dual-Band Reflection-Type Circular Polarizers Based on Anisotropic

Impedance Surfaces," *IEEE Trans. Antennas Propag.*, **64**, 2, pp. 826–830, 2016.

2. I. Sohail, Y. Ranga, K. P. Esselle, and S. G. Hay, "A linear to circular polarization converter based on jerusalem-cross frequency selective surface," *2013 7th Eur. Conf. Antennas Propag*., pp. 2141–2143, 2013.

3. H. Mirza, P. J. Soh, M. F. Jamlos, T. M. Hossain, M. N. Ramli, A. A. Al-Hadi, R. A. Sheikh, E. S. Hassan, and S. Yan, "A crossed dodecagonal deployable polarizer on textile and polydimethylsiloxane (PDMS) substrates," *Appl. Phys. A*, **124**, 2, p. 178, 2018.

4. H. X. Xu, G. M. Wang, J. G. Liang, M. Q. Qi, and X. Gao, "Compact circularly polarized antennas combining meta-surfaces and strong space-filling meta-resonators," *IEEE Trans. Antennas Propag*., **61**, 7, pp. 3442–3450, 2013.

5. H. X. Xu, S. Sun, S. Tang, S. Ma, Q. He, G. M. Wang, T. Cai, H. P. Li, and L. Zhou, "Dynamical control on helicity of electromagnetic waves by tunable metasurfaces," *Sci. Rep*., **6**, pp. 1–10, 2016.

6. L. Martinez-Lopez, J. Rodriguez-Cuevas, J. I. Martinez-Lopez, and A. E. Martynyuk, "A multilayer circular polarizer based on bisected split-ring frequency selective surfaces," *IEEE Antennas Wirel. Propag. Lett*., **13**, pp. 153–156, 2014.

7. E. Doumanis, G. Goussetis, J. L. Gómez-Tornero, R. Cahill, and V. Fusco, "Anisotropic impedance surfaces for linear to circular polarization conversion," *IEEE Trans. Antennas Propag*., **60**, 1, pp. 212–219, 2012.

8. W. Zhang, J. Li, and L. Wang, "Broadband Circular Polarizer Based on Multilayer Gradual Frequency Selective Surfaces," *Int. J. Antennas Propag*., pp. 1–5, 2016.

9. P. J. Soh, G. A. E. Vandenbosch, M. Mercuri, and D. M. M. P. Schreurs, "Wearable wireless health monitoring: Current developments, challenges, and future trends," *IEEE Microw. Mag*., **16**, 4, pp. 55–70, 2015.

10. S. Yan and G. A. E. Vandenbosch, "Compact circular polarizer based on chiral twisted double split-ring resonator," *Appl. Phys. Lett*., **102**, 10, pp. 1–5, 2013.

11. J. Wang, Z. Shen, W. Wu, and K. Feng, "Wideband circular polarizer based on dielectric gratings with periodic parallel strips," *Opt. Express*, **23**, 10, p. 12533, 2015.

12. CST-Computer Simulation Technology." [Online]. Available: https://www.cst.com/. [Accessed: 30-Mar-2018].

13. M. Hosseini and S. V. Hum, "A Circuit-Driven Design Methodology for a Circular Polarizer Based on Modified Jerusalem Cross Grids," *IEEE Trans. Antennas Propag*., **65**, 10, pp. 5322–5331, 2017.

14. M. Hosseini and M. Hakkak, "Characteristics Estimation for Jerusalem Cross-based Artificial Magnetic Conductors," *IEEE Antennas Wirel. Propag. Lett*., **7**, pp. 58–61, 2008.